PHYSICAL REVIEW E **68**, 025303(R) (2003)

Simple model for drag reduction

Roberto Benzi[1] and Itamar Procaccia[2,3]
[1]*Dipartimento di Fisica and INFM, Università "Tor Vergata," Via della Ricerca Scientifica 1, I-00133 Roma, Italy*
[2]*Department of Chemical Physics, The Weizmann Institute of Science, Rehovot 76100, Israel*
[3]*Centro Intranacional de Ciencias, UNAM, Cuernavaca, Mexico*
(Received 23 October 2002; published 18 August 2003)

Direct numerical simulations established that the finite-extension nonlinear-elasticity–Peterlin (FENE-P) model of viscoelastic flows exhibits the phenomenon of turbulent drag reduction which is caused in experiments by dilute polymeric additives. To gain analytic understanding of the phenomenon, we introduce in this paper a simple one-dimensional model of the FENE-P equations. We demonstrate drag reduction in the simple model, and explain analytically the main observations which include (i) reduction of velocity gradients for fixed throughput and (ii) increase of throughput for fixed dissipation.

DOI: 10.1103/PhysRevE.68.025303 PACS number(s): 47.27.Eq, 47.50.+d, 47.60.+i

The addition of few tens of parts per million (by weight) of long-chain polymers to turbulent fluids can bring about a reduction of the friction drag by up to 80% [1]. This "drag reduction" phenomenon has important practical implications besides being interesting from the fundamental point of view, integrating turbulence research with polymer physics. In spite of intense interest for an extended period of time [2–4], Sreenivasan and White [1] recently concluded that "it is fair to say that the extensive—and continuing—activity has not produced a firm grasp of the mechanisms of drag reduction." Recently, however, it was shown that drag reduction is observed in direct numerical simulation of model viscoelastic hydrodynamic equations [5–7]. From the theoretical viewpoint these observations are crucial, indicating that the phenomenon is included in the solutions of the model equations. Understanding drag reduction then becomes a usual challenge of theoretical physics. In this paper, we present a further simplification of the model equations and gain analytic insights into the phenomenon. The finite-extension nonlinear-elasticity–Peterlin (FENE-P) equation for the fluid velocity $\boldsymbol{u}(\boldsymbol{r},t)$ contains an additional stress tensor related to the polymer:

$$\frac{\partial \boldsymbol{u}}{\partial t}+(\boldsymbol{u}\cdot\boldsymbol{\nabla})\boldsymbol{u}=-\boldsymbol{\nabla}p+\nu_s\boldsymbol{\nabla}^2 u+\boldsymbol{\nabla}\cdot\boldsymbol{\mathcal{T}}+\boldsymbol{F}, \tag{1}$$

where ν_s is the viscosity of the neat fluid, $\boldsymbol{F}$ is the forcing, and the stress tensor $\boldsymbol{\mathcal{T}}$ is determined by the polymer conformation tensor $\boldsymbol{R}$ according to

$$\boldsymbol{\mathcal{T}}(\boldsymbol{r},t)=\frac{\nu_p}{\tau_p}\left[\frac{f(\boldsymbol{r},t)}{\rho_0^2}\boldsymbol{R}(\boldsymbol{r},t)-\mathbf{1}\right]. \tag{2}$$

Here, ν_p is a viscosity parameter, τ_p is a relaxation time for the polymer conformation tensor, ρ_0 is the rms extension of the polymers in equilibrium, and $f(\boldsymbol{r},t)$ is a function that limits the growth of the trace of $\boldsymbol{R}$. The model is closed by the equation of motion for the conformation tensor which reads

$$\frac{\partial R_{\alpha\beta}}{\partial t}+(\boldsymbol{u}\cdot\boldsymbol{\nabla})R_{\alpha\beta}=\frac{\partial u_\alpha}{\partial r_\gamma}R_{\gamma\beta}+R_{\alpha\gamma}\frac{\partial u_\gamma}{\partial r_\beta}-\frac{1}{\tau_p}[f(\boldsymbol{r},t)R_{\alpha\beta}-\rho_0^2\delta_{\alpha\beta}]. \tag{3}$$

These equations were simulated on the computer in a channel or pipe geometry. The main observations on the effect of the polymer on the turbulent flow that we need to focus on are the following.

(i) For a fixed pressure gradient at the wall the fluid throughput is increased (see Fig. 1).

(ii) For a fixed throughput the gradient at the wall decreases (i.e., the dissipation decreases).

(iii) The trace of the conformation tensor $\boldsymbol{R}$ follows qualitatively the rms streamwise velocity (see Fig. 2). We are particularly interested in point (iii) since in our opinion the space dependence of the amount of stretching (and with it of the effective viscosity) is crucial, and compare [8,9] for a discussion of this point in the context of the instability of laminar flows. Obviously, Eqs. (1)–(3) as they stand are not

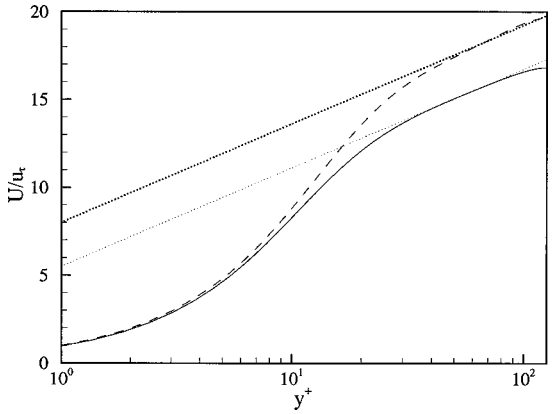

FIG. 1. The mean flow velocity as a function of the distance from the wall for the FENE-P (dashed line) vs the Newtonian flow (continuous line). The profiles hardly change near the wall, but the amplitude is larger for the FENE-P solution.

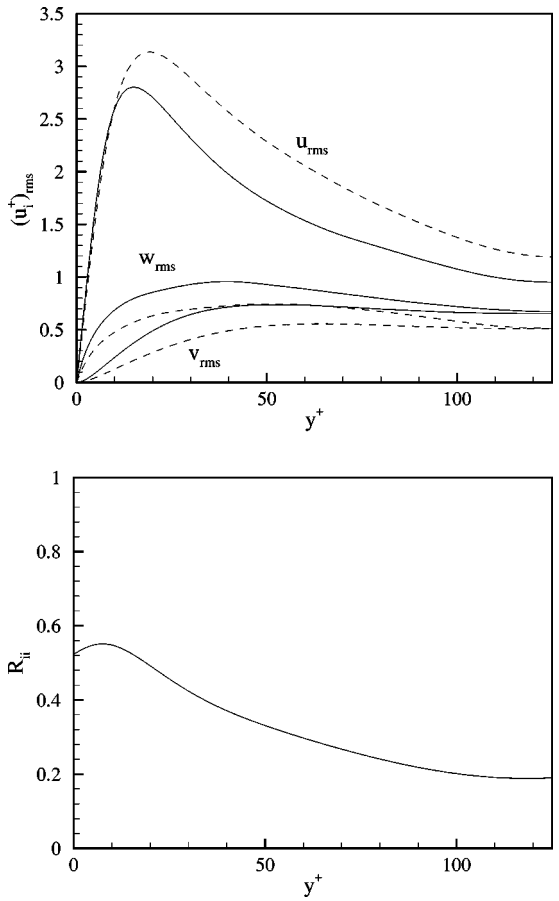

FIG. 2. Upper panel: the dependence of the rms velocity fluctuations as a function of the distance from the wall. We are interested in $U_{\rm rms}$ for comparison with our model. Lower panel: the trace of the conformation tensor $\boldsymbol{R}$ as a function of the distance from the wall. We stress the qualitative similarity to the dependence of $U_{\rm rms}$ in the upper panel.

amenable to analytic investigation in the turbulent regime. To gain insight, we therefore attempt to simplify them as much as possible without losing the main phenomena (i)–(iii). Consider therefore a model for the streamwise velocity which is the Burger's equation (u in the streamwise directions with gradients in the y (wall-normal) direction), to which the effect of a scalar R is added:

$$u_t + uu_y = \nu u_{yy} + sR_y + F, \tag{4}$$

$$R_t + uR_y = -\frac{1}{\tau}R + Ru_y, \tag{5}$$

where a subscript y stands for a partial derivative with respect to y. In the following, we shall denote Eqs. (4) and (5) with the acronimous *uR model*. The parameter s is related to the polymer concentration and τ is the relaxation time of R. We will consider the model in the domain $-L \leqslant y \leqslant L$, with boundary conditions chosen later. We will denote spatial averages by pointed brackets, $\langle A \rangle \equiv \int_{-L}^{L} A(y)dy$. The simplicity of the *uR* model allows us to state the energy budget in

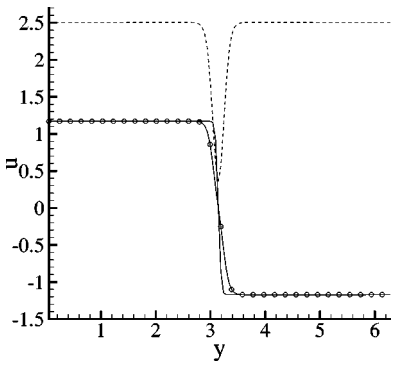

FIG. 3. Comparison of the solution of the *uR* model (connected circles) to the solution of Burger's equation (continuous line). The dashed line corresponds to the function R. The parameters are $\tau = 10^4$, $u_0 = 1.17$, $s = 0.25$, and $R_0 = 2.5$.

simple terms. Multiplying Eq. (4) by u and taking the spatial average of Eqs. (4) and (5), we obtain

$$\frac{1}{2}\frac{d}{dt}\langle u^2 \rangle = -\nu \langle u_y^2 \rangle + s\langle uR_y \rangle + \langle Fu \rangle, \tag{6}$$

$$\frac{d}{dt}\langle R \rangle = -\frac{1}{\tau}\langle R \rangle + 2\langle Ru_y \rangle. \tag{7}$$

The term $\langle uR_y \rangle$ measures the ''energy'' given by the velocity field u to the polymer field R. Multiplying Eq. (7) by $s/2$ and summing Eq. (7) with Eq. (6), we obtain

$$\frac{d}{dt}\left(\frac{1}{2}\langle u^2 \rangle + \frac{s}{2}\langle R \rangle \right) = -\nu \langle u_y^2 \rangle - \frac{s}{2\tau}\langle R \rangle + \langle Fu \rangle. \tag{8}$$

In the steady state, the overall power $\langle Fu \rangle$ is balanced by the overall energy dissipation per unit time D, $D = \nu \langle u_y^2 \rangle + (s/2\tau)\langle R \rangle$. The term $\frac{1}{2}\langle u^2 \rangle + (s/2)\langle R \rangle$ represents the sum of the kinetic energy of the flow plus the potential energy of the stretched polymers. We remark that already from these elementary considerations it becomes clear that for a fixed power input the existence of the term $(s/2\tau)\langle R \rangle$ necessarily reduces the gradients of u in agreement with point (ii) above. To address points (ii) and (iii) further, we consider next the solution of the model with $F = 0$ and with a fixed velocity u and stretching R at $-L$ and L. In other words, we take as boundary conditions

$$u(-L) = u_0, \quad u(L) = -u_0, \quad R(-L) = R(L) = R_0. \tag{9}$$

In Fig. 3, we compare the solution of the *uR* model to that of the pure Burger's equation [i.e., Eq. (4) with $R = F = 0$.] To focus our thinking, we would like the reader to consider the solution in the left half space as a model of the streamwise velocity component in the lower half channel, with the solution in the right half space being simply an antisymmetric copy. The position of the lateral ''wall'' is modeled by the point where $u = 0$. Thinking this way points (ii) and (iii) are clearly demonstrated. We proceed now analytically to demonstrate drag reduction [point (ii)] and to understand the pro-

file of R [point (iii)]. First, we consider the stationary solution of the pure Burger's equation. Integrate Eq. (4) in y to find

$$\tfrac{1}{2}u^2 = \nu u_y + \tfrac{1}{2}u_0^2, \tag{10}$$

where the constant of integration was fixed by noticing that for L sufficiently large u_y is expected to vanish at the boundaries. Multiplying Eq. (10) by u_y, and integrating between $-L$ and L using the boundary conditions, we find the viscous dissipation ϵ,

$$\epsilon \equiv \nu\langle u_x^2\rangle = \frac{2}{3}u_0^3. \tag{11}$$

Next we consider the solution of the uR model for the same boundary conditions (9) and $R \geqslant 0$. In the stationary state $R_t = 0$, and by dividing Eq. (5) by Ru we can integrate it formally in y and obtain

$$R = a|u|\exp\left(-\frac{1}{\tau}\int \frac{dy}{u}\right), \tag{12}$$

where a is a constant of integration. This equation is the explanation of point (iii). It says that for small velocity $u \sim 0$, i.e., for $y \sim 0$, R *necessarily goes to* 0. In particular, approximating $u = -my$ near the point $y = 0$, we obtain $R \sim |u|^b$, where $b = 1 + 1/(m\tau)$. Thus, we should expect that at positions with small u where the gradient of u is large the generic behavior of R is a cusp with $R = 0$ for $m\tau \geqslant 1$. To compute the dissipation analytically, we consider the limit $\tau \to \infty$, i.e., we look for a solution at the zero order of the perturbation series in $1/\tau$. In this limit

$$R = \frac{R_0}{u_0}|u|. \tag{13}$$

Returning to Eq. (4), we integrate it into y to obtain

$$\nu u_y = \tfrac{1}{2}u^2 - SR + sR_0 - \tfrac{1}{2}u_0^2. \tag{14}$$

We can now substitute Eq. (13) in the domain $-L \leqslant y \leqslant 0$ where $|u| = u$, and integrate between $-L$ and 0. Multiplying the result by a factor of 2, we find the viscous dissipation ϵ_R,

$$\epsilon_R = \tfrac{2}{3}\,u_0^3 - 3sR_0u_0\,. \tag{15}$$

This result is an analytic demonstration of point (ii). We note that our analysis has been performed in the limit $\tau \to \infty$. For large but finite values of τ, the qualitative picture we have drawn is unchanged. Needless to say, the above discussion can be reformulated by keeping constant the energy dissipation while increasing the value of u at the boundary, to demonstrate point (i). We choose, however, to demonstrate point (i) next, using a forced solution. Point (i) is most clearly demonstrated in the uR model using periodic boundary conditions and constant forcing. We consider $0 \leqslant y \leqslant 2\pi$ and choose the external forcing F to be

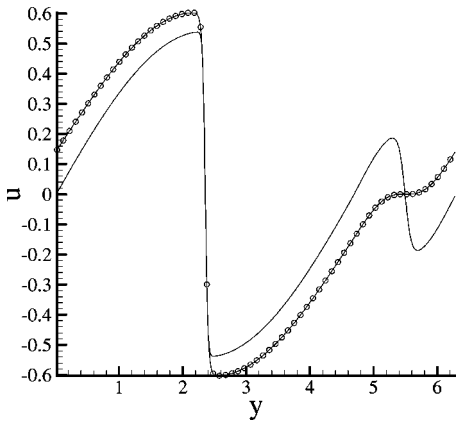

FIG. 4. The solution of the uR model with constant forcing and periodic boundary conditions (connceted circles). Continuous line: the Burger equation without the polymer.

$$F(y) = f_0 \sin(4y/3), \quad \text{for } 0 \leqslant y \leqslant \frac{3\pi}{2},$$

$$F(y) = f_1 \sin(4y), \quad \text{for } \frac{3\pi}{2} \leqslant y \leqslant 2\pi. \tag{16}$$

We examined the solutions of the uR model for the set of parameters $f_0 = 0.1$, $f_1 = 0.05$, $\nu = 0.01$, $s = 0.01$, and initial conditions $R(y) = 2\sin(y)$. The remaining parameter is the relaxation time τ. It turns out that for very small values of τ, no effect of the polymer field is observed. (We remark that for periodic boundary conditions the limit $\tau \to 0$ corresponds to the case of no polymer.) For $\tau \to \infty$ no stationary solutions can be obtained. For τ smaller than some critical value τ_c, the solution of the uR model shows stable stationary solutions with drag reduction. The typical situation is presented in Fig. 4, showing the numerical solutions for $\tau = (0.15)^{-1} \leqslant \tau_c$, compared against the solution of Burger's equation. The uR model shows a larger amplitude near the strongest shock due to forcing at $x = 3\pi/4$. It is worth noting that the gradient is maintained extremely close to the one obtained by the Burger equation, demonstrating nicely point (i). Point (iii) is nicely demonstrated in Fig. 5 which presents the solution for R together with u^2 for both the uR model and the Burger equation. As one can clearly see, the behavior of R is similar to what is observed in Fig. 1, namely, there is a qualitative similarity between the space dependence of R and u^2, here with a sharp cusp in R near the point of maximum gradient of u. On the other hand, the smallest shock present in the solution of Burger's equation has been completely smoothed out by the uR model. This is an indication that when R is not sufficiently suppressed where the gradient of u is significant, there can be *drag enhancement*. This important point will be addressed again in the concluding remarks. Again, the simplicity of the model affords an analytic explanation of why the solution near the biggest shock shows a larger velocity amplitude compared to the Burger equation. Let y_0 be the position of the maximal velocity near the shock. The position y_0 is unchanged in the two models. We can expand u, F, and R as power series near y_0. Let Δ be

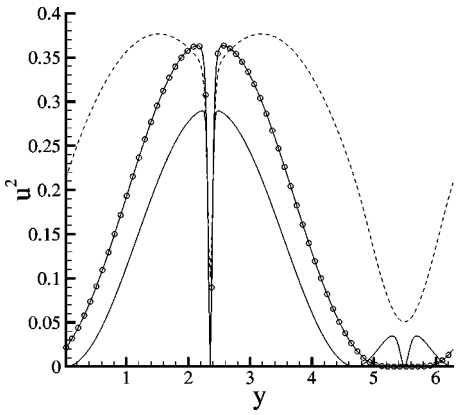

FIG. 5. The solution of the *uR* model with constant forcing and periodic boundary conditions. Dashed line: $R(y)$. Connected circles: $20u^2$ of the solution of *uR*. Solid line: $20u^2$ of the solution of Burger's equation.

defined as $\Delta = y_s - y_0$, where $y_s = 3\pi/4$ is where the velocity vanishes (the wall position in our model). We have

$$u(y) = u_0 - u_2 y^2, \quad F(y) = F_0 + F_1 y, \quad R(y) = R_0 + R_1 y, \tag{17}$$

where $F_0 \sim f_0 \Delta$ and $F_1 \sim -f_0$ because of Eq. (16). Inserting Eq. (17) into the *uR* model, we obtain

$$u_0 = \frac{\nu f_0 + s R_0 \tau^{-1}}{\Delta f_0} = u_b(1+P), \quad P = \frac{s R_0}{\nu \tau f_0}, \tag{18}$$

where $u_b = \nu/\Delta$ is the solution obtained without polymer ($P=0$). The increment of the velocity, which is responsible for the drag reduction, is proportional to sR_0.

In summary, we have introduced a simple model of the effect of polymeric additives to Newtonian fluids, with the aim of understanding in simple mathematical terms some of the prominent features associated with the phenomenon of drag reduction. Needless to say, the model cannot be taken as quantitative; we were concerned with the qualitative features summarized above for convenience as points (i)–(iii). We demonstrated that our model reproduces these qualitative features, and provided straightforward analytic explanation to all those features. It appears that we can draw from the results of this model a few important conclusions.

(i) Arguments concerning the turbulent cascade process do not appear essential. These arguments are the hallmark of the theory presented in Ref. [4] which proposed that the main effect of the polymer is to introduce a dissipative cutoff at scales larger than the Kolmogorov scale, due to the polymer relaxation time matching there the hydrodynamic time scale. Looking at Eq. (5), one could think that the largest velocity gradients could be estimated as $\langle |u_y| \rangle \sim 1/\tau$. But since R can go to 0 where the gradient is largest, such estimates cannot be made. Moreover, just an increase in the dissipative scale cannot account for drag reduction; a *homogeneous* increase in the effective viscosity should lead by itself to drag enhancement rather than reduction.

(ii) Drag reduction is a phenomenon that appears on the scales of the system size, involving energy containing modes rather than dissipative, small scale modes [10].

(iii) The main point appears to be the *space dependence* of the stretching of the polymer, here modeled by the value of $R(y)$. It is crucial that R is small where the velocity gradients are large. It is the space dependence of the effective viscosity which should be looked at as the source of drag reduction. A similar conclusion was arrived at in the context of the study of the stability of laminar flows in a channel geometry [8,9] accept that there the space dependence of the effective viscosity had been introduced by hand. In the FENE-P context as well as in our model (and presumably in actual experiments), the space dependence appears self-consistently. It remains to understand this self-consistent buildup of differential effective viscosity in the context of the much more elaborate FENE-P model. In light of the present results, this appears an extremely worthwhile endeavor that will shed important light on the phenomenon of drag reduction.

This work was supported in part by the European Commission under a TMR grant, the German Israeli Foundation, and the Naftali and Anna Backenroth-Bronicki Fund for Research in Chaos and Complexity. We thank E. de Angelis for Figs. 1 and 2, taken from her Ph.D. thesis.

[1] K.R. Sreenivasan and C.M. White, J. Fluid Mech. **409**, 149 (2000).
[2] J.L. Lumley, Annu. Rev. Fluid Mech. **1**, 367 (1969).
[3] P.S. Virk, AIChE J. **21**, 625 (1975).
[4] P.-G. de Gennes, *Introduction to Polymer Dynamics* (Cambridge University Press, Cambridge, 1990).
[5] J.M.J. de Toonder, M.A. Hulsen, G.D.C. Kuiken, and F.T.M. Nieuwstadt, J. Fluid Mech. **337**, 193 (1997).
[6] C.D. Dimitropoulos, R. Sureshdumar, and A.N. Beris, J. Non-Newtonian Fluid Mech. **79**, 433 (1998).
[7] E. de Angelis, C.M. Casciola, and R. Piva, CFD J. **9**, 1 (2000).
[8] R. Govindarajan, V.S. L'vov, and I. Procaccia, Phys. Rev. Lett. **87**, 174501 (2001).
[9] R. Govindarajan, V.S. L'vov, and I. Procaccia, Phys. Rev. E **67**, 026310 (2003).
[10] E. De Angelis, C.M. Casciola, V.S. L'vov, R. Piva, and I. Procaccia, Phys. Rev. E **67**, 056312 (2003).